

# OPEN-MAGVIT2: AN OPEN-SOURCE PROJECT TOWARD DEMOCRATIZ- ING AUTO-REGRESSIVE VISUAL GENERATION

Zhuoyan Luo<sup>1,2\*</sup> Fengyuan Shi<sup>1,3\*</sup> Yixiao Ge<sup>1†</sup> Yujiu Yang<sup>2</sup> Limin Wang<sup>3</sup> Ying Shan<sup>1</sup>

<sup>1</sup>ARC Lab, Tencent PCG

<sup>2</sup>Tsinghua University

<sup>3</sup>Nanjing University

<https://github.com/TencentARC/Open-MAGVIT2>



Figure 1: **Reconstruction and generation samples of Open-MAGVIT2.** We show  $1024 \times 1024$  reconstructed samples (top) and  $256 \times 256$  generated samples (middle and bottom).

## ABSTRACT

We present Open-MAGVIT2, a family of auto-regressive image generation models ranging from 300M to 1.5B. The Open-MAGVIT2 project produces an open-source replication of Google’s MAGVIT-v2 tokenizer, a tokenizer with a super-large codebook (i.e.,  $2^{18}$  codes), and achieves the state-of-the-art reconstruction performance (1.17 rFID) on ImageNet  $256 \times 256$ . Furthermore, we explore its application in plain auto-regressive models and validate scalability properties. To assist auto-regressive models in predicting with a super-large vocabulary, we factorize it into two sub-vocabulary of different sizes by asymmetric token factorization, and further introduce “next sub-token prediction” to enhance sub-token interaction for better generation quality. We release all models and codes to foster innovation and creativity in the field of auto-regressive visual generation.

\*Equal Contribution. Work done during an internship at ARC Lab, Tencent PCG.

†Corresponding author and project lead.

Table 1: **Model configurations of Open-MAGVIT2.** We partially follow the scaling rule proposed in the previous works (Sun et al., 2024; Tian et al., 2024).

Model	Parameters	Inter-Blocks $N$	Intra-Blocks $L$	Widths $w$	Heads $h$
Open-MAGVIT2-B	343M	24	2	1024	16
Open-MAGVIT2-L	804M	36	3	1280	20
Open-MAGVIT2-XL	1.5B	48	4	1536	24

## 1 INTRODUCTION

Large Language Models (LLMs), built upon auto-regressive transformer (Vaswani et al., 2017; OpenAI, 2023; Chowdhery et al., 2022; Touvron et al., 2023), have demonstrated dominance in natural language generation due to the incredible context modeling and scalability. Inspired by this, emergent works introduce auto-regressive models into visual generation (Van Den Oord et al., 2017; Esser et al., 2021; Yu et al., 2022; Lee et al., 2022; Sun et al., 2024). These approaches first utilize a vector quantizer for image tokenization and de-tokenization, then employ an auto-regressive transformer for discrete image token sequence modeling.

Although great processes are achieved, the quality of visual generation still falls behind the diffusion-based methods. The main factor is limited tokenizer performance. Tokenizers are generally posited as the upper bound of the visual generation, and inferior off-the-shelf tokenizers (e.g., VQ-VAE (Van Den Oord et al., 2017)) will lead to poor generation quality. Although some improvements are done (Yu et al., 2022; Lee et al., 2022; Sun et al., 2024), current tokenizers are limited by the codebook size and utilization, and the reconstruction performance is still far worse than VAE (Kingma, 2013; Rombach et al., 2022b) used in diffusion models. To unlock the potential of tokenizers, MAGVIT-v2 (Yu et al., 2024a) proposes Lookup-Free Quantizer to enable a highly code-activated and super-large codebook, and achieves better generation quality than diffusion models. **However, such a powerful visual tokenizer is completely closed-source and we have no access to this so far, limiting the development of the academic community.**

In this work, we push forward the auto-regressive visual generation in two folds: 1) **Replication of the visual tokenizer:** We re-implement the advanced Lookup-Free Quantizer proposed by MAGVIT-v2. To our best knowledge, our open-source replication achieves the closest reconstruction performance stated in MAGVIT-v2 (1.18 vs. 1.15 rFID on ImageNet 128×128) and outperforms all other methods on the hallmark Imagenet benchmark (Deng et al., 2009). 2) **Integrating a super-large codebook with AR visual generation:** Instead of simply following MAGVIT-v2 that leverages the vision-oriented design (i.e., mask generative methods (Chang et al., 2022) for visual synthesis), we seek to exploit the potential of such a large codebook in vanilla auto-regressive generation. To assist auto-regressive models in predicting with a super-large vocabulary, we factorize it into two sub-vocabulary of different sizes by asymmetric token factorization, and further introduce “next sub-token prediction” to enhance sub-token interaction for better generation quality. Our experiments on the standard visual generation dataset ImageNet suggest that, with the powerful tokenizer, the plain auto-regressive model exhibits superiority and scalability.

## 2 METHOD

### 2.1 OVERVIEW

Open-MAGVIT2 is composed of two significant stages. One is a powerful visual tokenizer that maps the input visual signal into the discrete token representations. Subsequently, the vector-quantized sequence will be fed into the auto-regressive transformer for intra- and inter-token relationship modeling, eventually for visual synthesis.

### 2.2 VISUAL TOKENIZER

**Preliminary.** Visual tokenization is fundamentally deemed as the crucial component in multi-modal large language models (MLLMs) to understand the visual signal input. The CNN-based

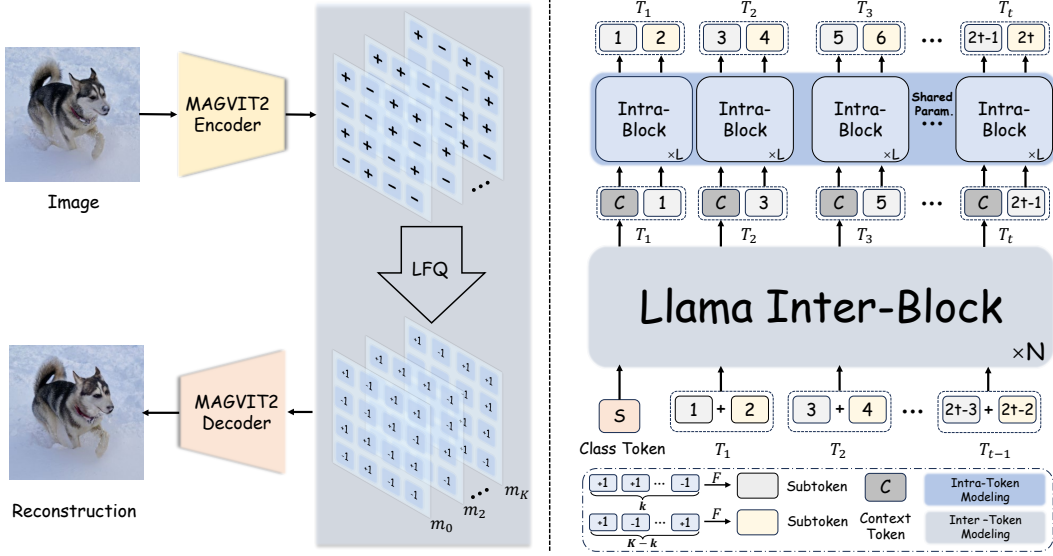


Figure 2: **Overview of Open-MAGVIT2.** There are two crucial stages in Open-MAGVIT2. In Stage I: the image is first encoded by MAGVIT-v2 Encoder and subsequently transformed into bits format by Lookup-Free Quantizer (LFQ). In Stage II: The quantized features are further mapped into discrete visual tokens and input into the Llama-based auto-regressive framework for intra- and inter-token relationship modeling.

encoder-quantizer-decoder architecture first proposed in VQVAE (Van Den Oord et al., 2017) is well adopted as the visual tokenizer, which maps input pixels into discrete representations and reconstructs images from quantized features. Specifically, given an image  $\mathcal{I} \in \mathbb{R}^{3 \times H \times W}$ , the encoder projects it into the feature map  $\mathcal{Z} \in \mathbb{R}^{D \times H' \times W'}$ , where  $H' = H/p$ ,  $W' = W/p$ , and  $p$  is the down-sample ratio. The quantizer containing a learnable codebook  $\mathcal{E} \in \mathbb{R}^{2^K \times D}$  then selects the closest entry  $\hat{z} \in \mathbb{R}^D$  from the codebook for each feature vector  $z \in \mathbb{R}^D$ . And we can use discrete token indices  $\mathcal{X} = \{x_i\}_{i=1}^{H' \times W'}$  to represent the continuous feature map  $\mathcal{Z}$ . For decoding, each code index will be mapped back to the quantized feature vector and input into the decoder for pixel-level image reconstruction.

**Review of Lookup-Free Quantization.** Motivated by the relationship between the size of the codebook and the dimension of code embeddings, MAGVIT-v2 (Yu et al., 2024a) eliminates the need for embedding lookup by reducing the dimension of code embedding to zero. Specifically, the codebook is shrunk into an integer set where the latent space of each entry is decomposed as the Cartesian product of single-dimensional variables (i.e.,  $\hat{\mathcal{C}} = \times_{i=1}^K \{-1, 1\}$ ,  $|\hat{\mathcal{C}}| = 2^K$ ). As shown in Fig. 2, the tokenization process can be simplified as:

$$\hat{z}_i = \text{sign}(z_i) = -\mathbb{1}\{z_i \leq 0\} + \mathbb{1}\{z_i > 0\}, \quad (1)$$

where  $\hat{z}_i$  denotes the quantized representation of the feature vector  $z_i$ . And the token index for  $z_i$  is given by:

$$\text{Index}(z_i) = \sum_{k=1}^K 2^{k-1} \mathbb{1}\{\hat{z}_{ik} > 0\}. \quad (2)$$

To encourage the confident assignment of each codebook entry and utilization of the whole codebook simultaneously, MAGVIT-v2 further introduces entropy loss:

$$\mathcal{L}_{\text{entropy}} = \frac{1}{BH'W'} \sum \mathbb{H}(f(z)) - \mathbb{H}\left(\frac{1}{BH'W'} \sum f(z)\right), \quad (3)$$

where  $\mathbb{H}(\cdot)$  denotes the entropy,  $B$  is batch sizes, and  $f(\cdot)$  is a mapping function from latent space to a categorical distribution specifying the probability of assignment to each entry. In our experiment, we observe that replacing traditional code assignment (i.e., pair-wise distance) with this lookup-free quantization enables training a super-large codebook (i.e.,  $2^{18}$  codes) of high utilization (100%).

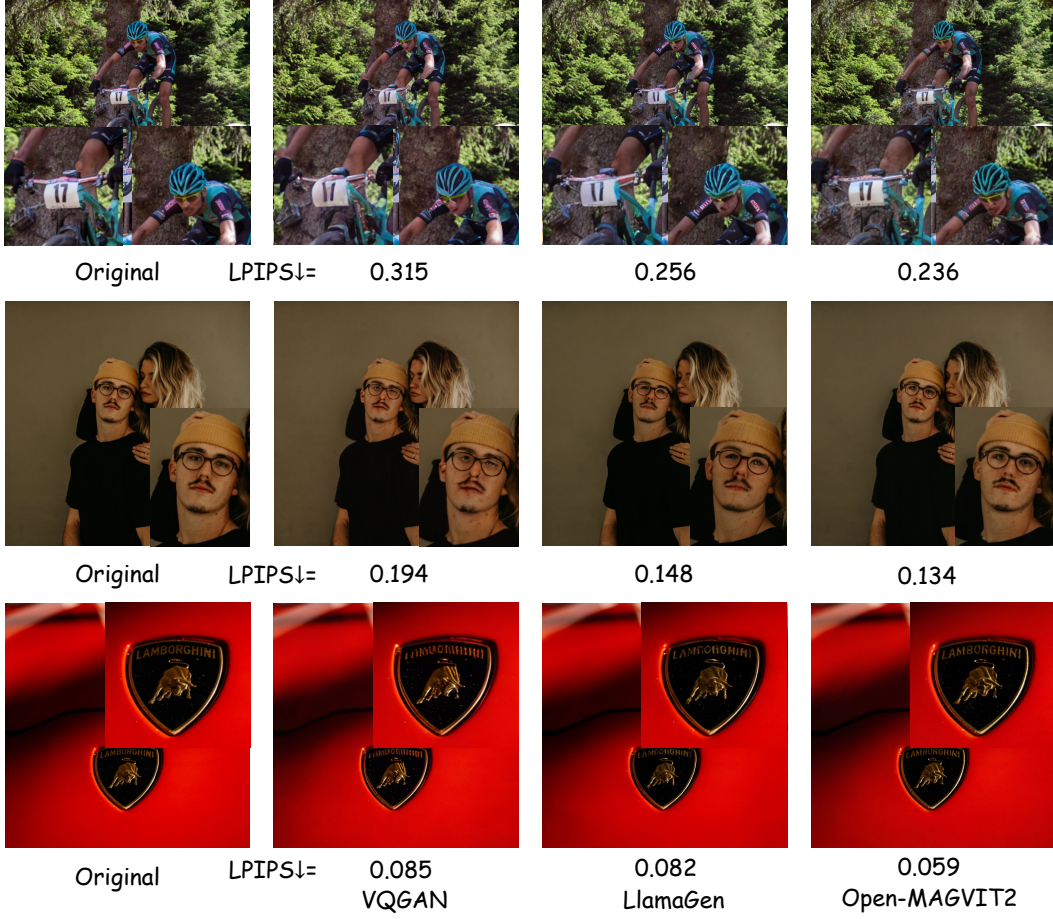


Figure 3: **Reconstruction comparison with different tokenizers.** We compare VQGAN (Esser et al., 2021), LlamaGen (Sun et al., 2024) and our models trained on ImageNet. (Best viewed with zooming in. The original images are from Unsplash).

**Review of Architecture improvements.** Intuitively, since each continuous feature vector will be quantized into  $K$  bits, it poses a significant challenge to both the encoder and decoder. Therefore, we re-implement the architecture improvements technique illustrated in (Yu et al., 2024a). 1) Downsamplers in the encoder are strided convolutions with learned kernels while upsamplers in the decoder are the depth-to-space operator. 2) Following (Karras et al., 2019; Peebles & Xie, 2023; Huang & Belongie, 2017), we re-implement the Adaptive GroupNorm Layer, which integrates the quantized vector with the output of each residual block in the decoder.

### 2.3 AUTO-REGRESSIVE TRANSFORMER

**Preliminary.** Given a sequence of discrete tokens  $\mathcal{X} = \{x_i\}_{i=1}^T, T = H' \times W'$  from the visual tokenizer, the auto-regressive transformer predicts the next token  $x_t$  conditioned on the previous tokens  $\{x_1, x_2, \dots, x_{t-1}\}$ :

$$p(x_1, x_2, \dots, x_T) = \prod_{t=1}^T p(x_t | x_1, x_2, \dots, x_{t-1}). \quad (4)$$

**Auto-regressive Architecture.** Considering the different scales of auto-regressive transformer (i.e., from  $\sim 300M$  to  $1B$ ) and the limited training academic data, directly optimizing such a large vocabulary (i.e.,  $2^{18}$  codes) is impractical. Therefore, we propose the asymmetric token factorization technique to assist models in performing “next-token prediction” within concatenated codebooks. Specifically, the LFQ token’s latent space is factorized into  $M$  subspaces  $\{x_i^1\}_{i=1}^T, \{x_i^2\}_{i=1}^T, \dots$ ,

$\{x_i^M\}_{i=1}^T$ , each of which contains  $2^{k_m}$  tokens. As shown in Fig. 2, each subspace is embedded individually and their summation is used as the transformer inputs. Conventionally, an intuitive solution to perform auto-regressive within subspaces is leveraging  $M$  separate heads for independent categorical distribution modeling. However, since both sub-tokens are derived from the same latent spaces, such a simple operation may ignore their intra-correlation. Consequently, inspired by (Lee et al., 2022), we reformulate the autoregression paradigm into modeling both intra- and inter-token dependency, which is essentially “next sub-token prediction”. In this manner, the representational capacity of the super-large codebook can exhibit great potential in auto-regressive generation with better scalability.

1) **Inter-token Relationship**: Given a set of sub-tokens from the visual tokenizers, a stacked of Llama blocks with  $N$  layers and  $w$  width are leveraged to capture the in-context information between tokens. The process can be formulated as:

$$\mathcal{C}_t = \text{LlamaBlock}(s, (\sum_{i=1}^M x_1^i), \dots, (\sum_{i=1}^M x_{t-1}^i)), \quad (5)$$

where  $s$  denotes the conditional tokens,  $\mathcal{C}_t \in \mathbb{R}^{T \times w_s}$  is the  $t$ -th context token.

2) **Intra-token Relationship**: We further utilize a transformer with  $L$  intra-blocks to autoregressively predict the each sub-token  $(x_t^1, x_t^2, \dots, x_t^M)$  at the position  $t$ . By associating the sub-token conditioned with contextual-enriched vector  $\mathcal{C}$ , the intra-dependency within tokens can be well modeled. Formally, at  $t$  position, the autoregression of predicting the conditional distribution of each sub-token is:

$$p_{tm} = \text{LlamaBlock}(\mathcal{C}_t, x_t^1 \dots, x_t^{m-1}). \quad (6)$$

Therefore, the auto-regressive likelihood is formulated as:

$$\begin{aligned} p(X_1, X_2, \dots, X_T) &= \prod_{t=1}^T p(X_t | X_1, X_2, \dots, X_{t-1}) \\ &= \prod_{t=1}^T \prod_{m=1}^M p(x_t^m | (X_1, X_2, \dots, X_{t-1}), (x_t^1, x_t^2, \dots, x_t^{m-1})), \end{aligned} \quad (7)$$

where  $X_t$  specifies a set of sub-token  $\{x_t^1, x_t^2, \dots, x_t^M\}$  at each position  $t$ .

### 3 EXPERIMENTS

#### 3.1 DATASET AND METRICS

The training of the visual tokenizer and auto-regressive transformer are both on ImageNet (Deng et al., 2009). Specifically, we train the tokenizer in  $128 \times 128$  and  $256 \times 256$  resolutions.

For visual reconstruction, the reconstruction-FID, denoted as rFID (Heusel et al., 2017), codebook utilization, the use percentage of codes, and PSNR on ImageNet 50k validation set are adopted to measure the quality of reconstructed images. Simultaneously, we measure the quality of image generation by the prevalent metrics FID, IS (Salimans et al., 2016) and Precision/Recall (Kynkänniemi et al., 2019).

#### 3.2 IMPLEMENTATIONS DETAILS

**Visual Tokenizer Setup.** Open-MAGVIT2 follows the same architecture of the visual tokenizer proposed in (Yu et al., 2024a). For computational efficiency, we remove the gradient penalty loss, and adopt PatchGAN (Isola et al., 2017) as the discriminator instead of StyleGAN (Karras et al., 2019). All models corresponding to different resolutions are trained with similar settings: an initial  $1e-4$  learning rate, an Adam Optimizer with  $\beta_1 = 0.5$ ,  $\beta_2 = 0.9$ , a total 256 batch size from 270 to 350 epochs, a combination of reconstruction, GAN, perceptual (Zhang et al., 2018), entropy penalty (Yu et al., 2024a), commitment losses, LeCAM regularization (Tseng et al., 2021) for training stability, and  $32 \times$  Nvidia V100 / Ascend 910B with Pytorch.

Table 2: Model designs and reconstruction performance comparison with the original MAGVIT-v2 on  $128 \times 128$  ImageNet 50k validation set, following the MAGVIT-v2 paper.

Method	Tokens	Train Resolution	LFQ	Large Codebook	Up/Down Sampler	Deeper Model	Adaptive GroupNorm	rFID
Open-MAGVIT2	$16 \times 16$	$128 \times 128$	✓	✓	✓	✓	✓	1.18
MAGVIT2 (Yu et al., 2024a)	$16 \times 16$	$128 \times 128$	✓	✓	✓	✓	✓	1.15

Table 3: Reconstruction performance of different tokenizers on  $256 \times 256$  ImageNet 50k validation set. Open-MAGVIT2 achieves SOTA results on different downsampling rates.  $\dagger$  specifies that the training is on OpenImages.  $*$  denotes that the results are from the direct inference using the model trained with  $128 \times 128$  resolution without fine-tuning.

Method	Token Type	Tokens	Ratio	Train Resolution	Codebook Size	rFID $\downarrow$	PSNR $\uparrow$	Codebook Usage $\uparrow$
VQGAN (Esser et al., 2021)	2D	$16 \times 16$	16	$256 \times 256$	1024	7.94	19.4	—
SD-VQGAN (Rombach et al., 2022a)	2D	$16 \times 16$	16	$256 \times 256$	16384	5.15	—	—
MaskGIT (Chang et al., 2022)	2D	$16 \times 16$	16	$256 \times 256$	1024	2.28	—	—
LlamaGen (Sun et al., 2024)	2D	$16 \times 16$	16	$256 \times 256$	16384	2.19	20.79	97%
<b>Open-MAGVIT2</b>	2D	$16 \times 16$	16	$256 \times 256$	262144	<b>1.17</b>	<b>21.90</b>	<b>100%</b>
ViT-VQGAN (Yu et al., 2022)	2D	$32 \times 32$	8	$256 \times 256$	8192	1.28	—	—
VQGAN $\dagger$ (Esser et al., 2021)	2D	$32 \times 32$	8	$256 \times 256$	16384	1.19	23.38	—
SD-VQGAN $\dagger$ (Rombach et al., 2022a)	2D	$32 \times 32$	8	$256 \times 256$	16384	1.14	—	—
OmiTokenizer-VQ (Wang et al., 2024)	2D	$32 \times 32$	8	$256 \times 256$	8192	1.11	—	—
LlamaGen (Sun et al., 2024)	2D	$32 \times 32$	8	$256 \times 256$	16384	0.59	24.45	—
<b>Open-MAGVIT2<math>*</math></b>	2D	$32 \times 32$	8	$128 \times 128$	262144	<b>0.34</b>	<b>26.19</b>	<b>100%</b>
Titok-L (Yu et al., 2024b)	1D	32	—	$256 \times 256$	4096	2.21	—	—
Titok-B (Yu et al., 2024b)	1D	64	—	$256 \times 256$	4096	1.70	—	—
Titok-S (Yu et al., 2024b)	1D	128	—	$256 \times 256$	4096	1.71	—	—

**Auto-regressive Transformer Setup.** As illustrated, we propose asymmetric token factorization to assist the auto-regressive transformer models in making the precise prediction with a large codebook. Note that, we empirically set  $M = 2$  and  $k_1 = 6$ ,  $k_2 = 12$ . Since our main focus is on democratizing scalable auto-regressive visual generation, the plain auto-regressive transformer is utilized while the techniques that introduce inductive bias such as AdaLn (Karras et al., 2020) are excluded. Specifically, we adopt the Llama-based (Touvron et al., 2023) architecture (e.g., RoPE (Su et al., 2024), SwiGLU (Shazeer, 2020), RMSNorm (Zhang et al., 2022) technique, each of which has been proven effective in (Sun et al., 2024)). The class embedding which is indexed from a set of learnable embeddings serves as the start token. Open-MAGVIT2 follows the simple scaling principle proposed in (Sun et al., 2024), which is in Tab. 1. All models are trained with similar settings: a base learning rate of  $1e-4$  per 256 batch size, an AdamW optimizer with  $\beta_1 = 0.9$ ,  $\beta_2 = 0.95$ , weight decay =  $5e-2$ , a total 768 batch size and  $300 \sim 350$  training epochs, gradient clipping of 1.0, 0.1 dropout rate for input embedding, FFN module and conditional embedding, 32  $\sim$  96  $\times$  Nvidia V100 / Ascend 910B for different scales of the model with Pytorch.

### 3.3 MAIN RESULTS

**Visual Reconstruction.** As shown in Tab. 2, by incorporating all useful designs proposed in (Yu et al., 2024a), Open-MAGVIT2 matches MAGVIT-v2 performances with merely 0.03 FID margin on ImageNet  $128 \times 128$ . Further, we also compare our Open-MAGVIT2 with previous visual tokenizers on ImageNet  $256 \times 256$  in Tab. 3. Benefiting from the super-large codebook with lookup-free quantization, Open-MAGVIT2 outperforms all previous image tokenizers under fair settings. Moreover, we provide an illustrative visual comparison in Fig. 3. As indicated, our visual tokenizer gains more superiority in detail perception as well as precise facial and text reconstruction.

**Visual Generation.** MAGVIT-v2 leverages the non-autoregressive framework for image synthesis and achieves competitive performance. Considering the scalability of auto-regressive models and the remarkable success of the auto-regressive paradigm in MLLM (Team, 2024), we instead focus on exploring the potential of incorporating a super-large codebook for auto-regressive visual generation.

Table 4: Class-conditional generation on  $256 \times 256$  ImageNet. \* specifies the generated images are  $384 \times 384$  and are resized to  $256 \times 256$  for evaluation. The evaluation protocol and implementation are the same with ADM.

Type	Model	#Para.	FID $\downarrow$	IS $\uparrow$	Precision $\uparrow$	Recall $\uparrow$
Diffusion	ADM (Dhariwal & Nichol, 2021)	554M	10.94	101.0	0.69	0.63
	CDM (Ho et al., 2022)	—	4.88	158.7	—	—
	LDM-4 (Rombach et al., 2022a)	400M	3.60	247.7	—	—
	DiT-XL/2 (Peebles & Xie, 2023)	675M	2.27	278.2	0.83	0.57
AR	VQGAN (Esser et al., 2021)	227M	18.65	80.4	0.78	0.26
	VQGAN (Esser et al., 2021)	1.4B	15.78	74.3	—	—
	VQGAN-re (Esser et al., 2021)	1.4B	5.20	280.3	—	—
	ViT-VQGAN (Yu et al., 2022)	1.7B	4.17	175.1	—	—
	ViT-VQGAN-re (Yu et al., 2022)	1.7B	3.04	227.4	—	—
	RQTran. (Lee et al., 2022)	3.8B	7.55	134.0	—	—
	RQTran.-re (Lee et al., 2022)	3.8B	3.80	323.7	—	—
VAR	VAR-d16 (Tian et al., 2024)	310M	3.30	274.4	0.84	0.51
	VAR-d20 (Tian et al., 2024)	600M	2.57	302.6	0.83	0.56
	VAR-d24 (Tian et al., 2024)	1.0B	2.09	312.9	0.82	0.59
	VAR-d30 (Tian et al., 2024)	2.0B	1.92	323.1	0.82	0.59
AR	LlamaGen-L* (Sun et al., 2024)	343M	3.07	256.06	0.83	0.52
	LlamaGen-XL* (Sun et al., 2024)	775M	2.62	244.08	0.80	0.57
	LlamaGen-XXL* (Sun et al., 2024)	1.4B	2.34	253.90	0.80	0.59
	LlamaGen-L (Sun et al., 2024)	343M	3.80	248.28	0.83	0.51
	LlamaGen-XL (Sun et al., 2024)	775M	3.39	227.08	0.81	0.54
	LlamaGen-XXL (Sun et al., 2024)	1.4B	3.09	253.61	0.83	0.53
	Open-MAGVIT2-B	343M	3.08	258.26	0.85	0.51
	Open-MAGVIT2-L	804M	2.51	271.70	0.84	0.54
	Open-MAGVIT2-XL	1.5B	2.33	271.77	0.84	0.54

As shown in Tab. 4, Open-MAGVIT2 outperforms all previous image generation models using a plain auto-regressive approach. This benefits from the increased representational capacity of the large scale of the codebook. However, we believe that the strength of such a large codebook is still underestimated because of the data bottleneck and the model size. We hope our effort in building such a powerful visual tokenizer helps merit future research in unified MLLM for image generation.

### 3.4 QUALITATIVE RESULTS

We present the qualitative results on Imagenet Benchmark in terms of visual reconstruction (see in Fig. 4) and visual generation (see in Fig. 5), respectively.

## 4 RELATED WORKS

### 4.1 VISUAL TOKENIZER

Visual tokenizer is to map an image into compact discrete tokens, which are subsequently fed into the generative models for sequence modeling. Early pioneer VQVAE (Van Den Oord et al., 2017) first introduces learnable codebook mechanism for 2D tokens generation. Subsequently, ViT-VQGAN (Yu et al., 2022) and RQ-VAE (Lee et al., 2022) improve VQVAE through normalized and multi-scale quantization respectively. Recently, LlamaGen (Sun et al., 2024) reexamines the design of vanilla tokenizer (Esser et al., 2021) and reveals the conflict between the fidelity of the synthesized image and the size of codebook. Therefore, following the simple intuition (Yu et al., 2022) that reducing code dimension limits the representational capacity of individual tokens, MAGVIT-2 (Yu et al., 2024a) proposes an advanced visual tokenizer which significantly enlarges the size of codebook to  $2^{18}$  with Lookup-Free Quantization.

## 4.2 VISUAL GENERATION

Given a set of compact discrete image tokens, there exist two prevalent frameworks for the subsequent image synthesis, including Non-autoregressive and Auto-regressive generation.

**Non-autoregressive frameworks.** MaskGIT (Chang et al., 2022) utilizes BERT-style transformer (Devlin et al., 2018) to parallelly generate all visual tokens via masked-prediction mechanism. MAGVIT (Yu et al., 2023; 2024a) adopts the same architecture but includes an additional embedding mask for better generation quality.

**Auto-regressive frameworks.** Autoregressive-based Multi-Modal Large Language Models (Liu et al., 2024; Li et al., 2024) has achieved remarkable success in versatile visual understanding. In contrast, the progress in counterpart visual generation still remains unsatisfactory. The simplest approach VQGAN (Esser et al., 2021) employs tiny GPT2 (Radford et al., 2019) ( $\sim 300M$ ) for next-token prediction. VAR (Tian et al., 2024) reformulates the image generation approach into next-scale prediction and unveils the scaling principle simultaneously. Subsequently, LlamaGen (Sun et al., 2024) extends VQGAN with Llama (Touvron et al., 2023) architecture, showcasing significant improvement in fidelity. However, the limited codebook size (e.g.,  $2^{14}$ ) in existing auto-regressive models may incur the representational bottleneck. Therefore, considering that the capacity of the visual tokenizer is highly correlated with the quality of visual synthesis (Yu et al., 2024a), we democratize the plain auto-regressive approach with a super-large codebook.

## 5 CONCLUSION

In this work, we re-implement the powerful visual tokenizer, which achieves state-of-the-art performance compared with previous methods, and make it available to the community. Instead of simply following (Yu et al., 2024a) that leverages masked-generative transformer for visual generation, we delve into a more promising manner (i.e., auto-regressive visual synthesis). To excavate the potential of the large vocabulary, we introduce the “next sub-token prediction” paradigm with the asymmetric token factorization technique. The experiment suggests that with the powerful tokenizer, the plain auto-regressive model exhibits superiority and scalability. We hope our contribution to the open-source community can facilitate more innovative and creative works in the field of auto-regressive visual generation, eventually making a difference in building an omnipotent multi-modal framework.

**Limitations and future work.** We expect that the effectiveness of such a super-large codebook, (i.e.,  $2^{18}$  codes), is still underestimated due to the limited data scale and the sacrifice of the representational capacity with the token factorization technique. We believe that by amplifying the task with more training data (e.g., text-conditional image generation, video generation, etc.), and enlarging the model size to 7B or even larger, the potential of AR generation with a super-large codebook can be dramatically exploited. Therefore, extending Open-MAGVIT2 into more broad multi-modal generation applications will be a high priority in our future exploration.

## ACKNOWLEDGMENTS

We sincerely thank Lijun Yu for his encouraging discussions and support. We also thank Tianheng Cheng and Yuxin Chen for their helpful suggestions on this project.



Figure 4: **Visualization of the Open-MAGVIT2 tokenizer.** The upper part illustrates the model trained at  $128 \times 128$  resolution and tested at  $512 \times 512$  resolution. The second part showcases the tokenizer trained at  $256 \times 256$  resolution and tested at  $256 \times 256$  resolution. (a) indicates the original images while (b) specifies the reconstruction images.

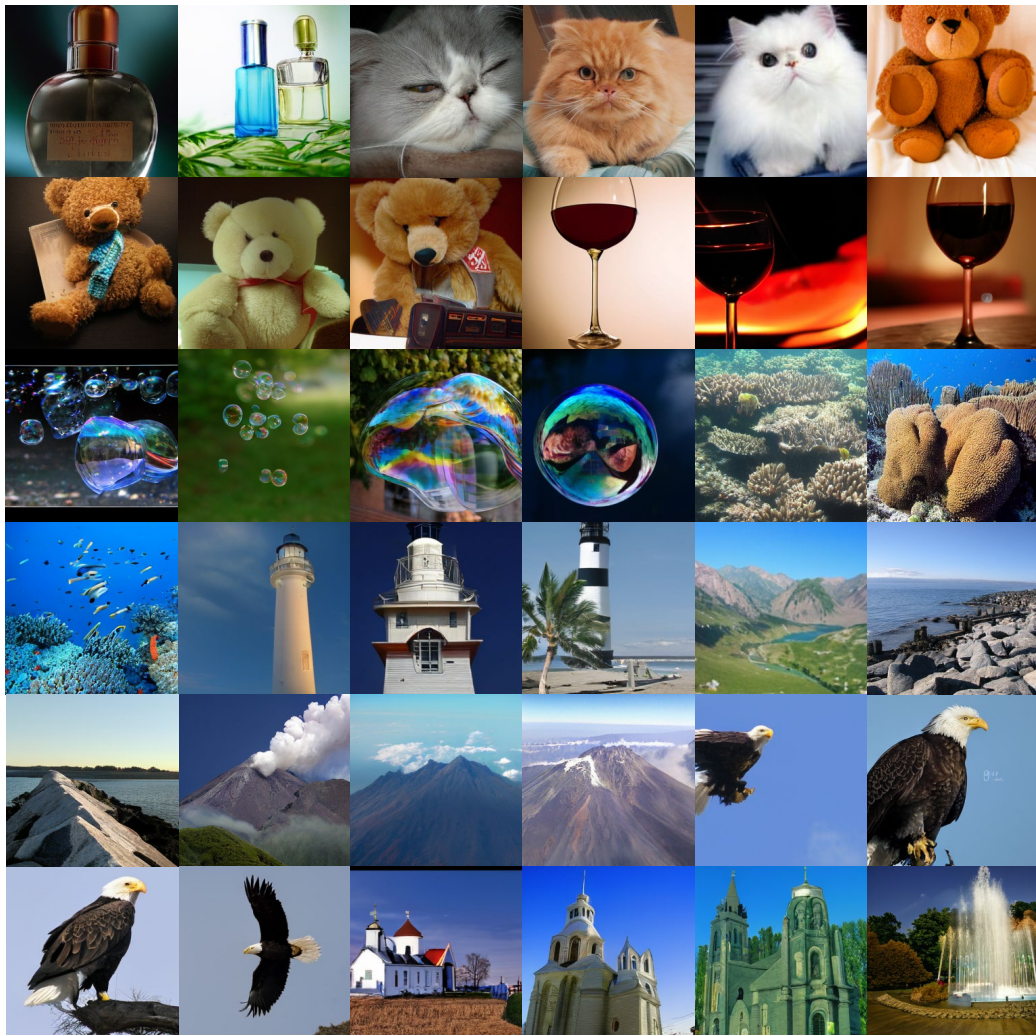


Figure 5: **Visualization of Open-MAGVIT2 auto-regressive generations.** Class-conditional generation on ImageNet 256 × 256.

## REFERENCES

Huiwen Chang, Han Zhang, Lu Jiang, Ce Liu, and William T. Freeman. Maskgit: Masked generative image transformer. In *CVPR*, pp. 11305–11315, 2022. [2](#), [6](#), [8](#)

Aakanksha Chowdhery, Sharan Narang, Jacob Devlin, Maarten Bosma, Gaurav Mishra, Adam Roberts, Paul Barham, Hyung Won Chung, Charles Sutton, Sebastian Gehrmann, et al. PaLM: Scaling language modeling with pathways. *arXiv preprint arXiv:2204.02311*, 2022. [2](#)

Jia Deng, Wei Dong, Richard Socher, Li-Jia Li, Kai Li, and Li Fei-Fei. ImageNet: A large-scale hierarchical image database. In *CVPR*, pp. 248–255, 2009. [2](#), [5](#)

Jacob Devlin, Ming-Wei Chang, Kenton Lee, and Kristina Toutanova. Bert: Pre-training of deep bidirectional transformers for language understanding. *arXiv preprint arXiv:1810.04805*, 2018. [8](#)

Prafulla Dhariwal and Alexander Nichol. Diffusion models beat gans on image synthesis. *NeurIPS*, 34:8780–8794, 2021. [7](#)

Patrick Esser, Robin Rombach, and Björn Ommer. Taming transformers for high-resolution image synthesis. In *CVPR*, pp. 12873–12883, 2021. [2](#), [4](#), [6](#), [7](#), [8](#)

Martin Heusel, Hubert Ramsauer, Thomas Unterthiner, Bernhard Nessler, and Sepp Hochreiter. GANs trained by a two time-scale update rule converge to a local nash equilibrium. In *NeurIPS*, volume 30, 2017. [5](#)

Jonathan Ho, Chitwan Saharia, William Chan, David J Fleet, Mohammad Norouzi, and Tim Salimans. Cascaded diffusion models for high fidelity image generation. *JMLR*, 23(1):2249–2281, 2022. [7](#)

Xun Huang and Serge J. Belongie. Arbitrary style transfer in real-time with adaptive instance normalization. In *ICCV*, pp. 1510–1519, 2017. [4](#)

Phillip Isola, Jun-Yan Zhu, Tinghui Zhou, and Alexei A. Efros. Image-to-image translation with conditional adversarial networks. In *CVPR*, pp. 5967–5976, 2017. [5](#)

Tero Karras, Samuli Laine, and Timo Aila. A style-based generator architecture for generative adversarial networks. In *CVPR*, pp. 4401–4410, 2019. [4](#), [5](#)

Tero Karras, Samuli Laine, Miika Aittala, Janne Hellsten, Jaakko Lehtinen, and Timo Aila. Analyzing and improving the image quality of stylegan. In *CVPR*, pp. 8110–8119, 2020. [6](#)

Diederik P Kingma. Auto-encoding variational bayes. *arXiv preprint arXiv:1312.6114*, 2013. [2](#)

Tuomas Kynkänniemi, Tero Karras, Samuli Laine, Jaakko Lehtinen, and Timo Aila. Improved precision and recall metric for assessing generative models. In Hanna M. Wallach, Hugo Larochelle, Alina Beygelzimer, Florence d’Alché-Buc, Emily B. Fox, and Roman Garnett (eds.), *NeurIPS*, pp. 3929–3938, 2019. [5](#)

Doyup Lee, Chiheon Kim, Saehoon Kim, Minsu Cho, and Wook-Shin Han. Autoregressive image generation using residual quantization. In *CVPR*, pp. 11513–11522, 2022. [2](#), [5](#), [7](#)

Yanwei Li, Yuechen Zhang, Chengyao Wang, Zhisheng Zhong, Yixin Chen, Ruihang Chu, Shaoteng Liu, and Jiaya Jia. Mini-gemini: Mining the potential of multi-modality vision language models. *arXiv preprint arXiv:2403.18814*, 2024. [8](#)

Haotian Liu, Chunyuan Li, Qingyang Wu, and Yong Jae Lee. Visual instruction tuning. *Advances in neural information processing systems*, 36, 2024. [8](#)

OpenAI. GPT-4 technical report. *arXiv preprint arXiv:2303.08774*, 2023. [2](#)

William Peebles and Saining Xie. Scalable diffusion models with transformers. In *CVPR*, pp. 4195–4205, 2023. [4](#), [7](#)

Alec Radford, Jeffrey Wu, Rewon Child, David Luan, Dario Amodei, Ilya Sutskever, et al. Language models are unsupervised multitask learners. *OpenAI Blog*, 2019. [8](#)

Robin Rombach, Andreas Blattmann, Dominik Lorenz, Patrick Esser, and Björn Ommer. High-resolution image synthesis with latent diffusion models. In *CVPR*, pp. 10684–10695, 2022a. 6, 7

Robin Rombach, Andreas Blattmann, Dominik Lorenz, Patrick Esser, and Björn Ommer. High-resolution image synthesis with latent diffusion models. In *CVPR*, pp. 10674–10685, 2022b. 2

Tim Salimans, Ian Goodfellow, Wojciech Zaremba, Vicki Cheung, Alec Radford, and Xi Chen. Improved techniques for training gans. In *NeurIPS*, volume 29, 2016. 5

Noam Shazeer. Glu variants improve transformer. *arXiv preprint arXiv:2002.05202*, 2020. 6

Jianlin Su, Murtadha Ahmed, Yu Lu, Shengfeng Pan, Wen Bo, and Yunfeng Liu. Roformer: Enhanced transformer with rotary position embedding, 2024. 6

Peize Sun, Yi Jiang, Shoufa Chen, Shilong Zhang, Bingyue Peng, Ping Luo, and Zehuan Yuan. Autoregressive model beats diffusion: Llama for scalable image generation. *arXiv preprint arXiv:2406.06525*, 2024. 2, 4, 6, 7, 8

Chameleon Team. Chameleon: Mixed-modal early-fusion foundation models. *arXiv preprint arXiv:2405.09818*, 2024. 6

Keyu Tian, Yi Jiang, Zehuan Yuan, Bingyue Peng, and Liwei Wang. Visual autoregressive modeling: Scalable image generation via next-scale prediction. *arXiv preprint arXiv:2404.02905*, 2024. 2, 7, 8

Hugo Touvron, Louis Martin, Kevin Stone, Peter Albert, Amjad Almahairi, Yasmine Babaei, Niko lay Bashlykov, Soumya Batra, Prajjwal Bhargava, Shruti Bhosale, Dan Bikel, Lukas Blecher, Cristian Canton-Ferrer, Moya Chen, Guillem Cucurull, David Esiobu, Jude Fernandes, Jeremy Fu, Wenyin Fu, Brian Fuller, Cynthia Gao, Vedanuj Goswami, Naman Goyal, Anthony Hartshorn, Saghar Hosseini, Rui Hou, Hakan Inan, Marcin Kardas, Viktor Kerkez, Madian Khabsa, Isabel Kloumann, Artem Korenev, Punit Singh Koura, Marie-Anne Lachaux, Thibaut Lavril, Jenya Lee, Diana Liskovich, Yinghai Lu, Yuning Mao, Xavier Martinet, Todor Mihaylov, Pushkar Mishra, Igor Molybog, Yixin Nie, Andrew Poulton, Jeremy Reizenstein, Rashi Rungta, Kalyan Saladi, Alan Schelten, Ruan Silva, Eric Michael Smith, Ranjan Subramanian, Xiaoqing Ellen Tan, Binh Tang, Ross Taylor, Adina Williams, Jian Xiang Kuan, Puxin Xu, Zheng Yan, Iliyan Zarov, Yuchen Zhang, Angela Fan, Melanie Kambadur, Sharan Narang, Aurélien Rodriguez, Robert Stojnic, Sergey Edunov, and Thomas Scialom. Llama 2: Open foundation and fine-tuned chat models. *arXiv preprint arXiv:2307.09288*, 2023. 2, 6, 8

Hung-Yu Tseng, Lu Jiang, Ce Liu, Ming-Hsuan Yang, and Weilong Yang. Regularizing generative adversarial networks under limited data. In *CVPR*, pp. 7921–7931, 2021. 5

Aaron Van Den Oord, Oriol Vinyals, et al. Neural discrete representation learning. volume 30, 2017. 2, 3, 7

Ashish Vaswani, Noam Shazeer, Niki Parmar, Jakob Uszkoreit, Llion Jones, Aidan N. Gomez, Łukasz Kaiser, and Illia Polosukhin. Attention is all you need. In Isabelle Guyon, Ulrike von Luxburg, Samy Bengio, Hanna M. Wallach, Rob Fergus, S. V. N. Vishwanathan, and Roman Garnett (eds.), *NeurIPS*, pp. 5998–6008, 2017. 2

Junke Wang, Yi Jiang, Zehuan Yuan, Binyue Peng, Zuxuan Wu, and Yu-Gang Jiang. Omnitokenizer: A joint image-video tokenizer for visual generation. *arXiv preprint arXiv:2406.09399*, 2024. 6

Jiahui Yu, Xin Li, Jing Yu Koh, Han Zhang, Ruoming Pang, James Qin, Alexander Ku, Yuanzhong Xu, Jason Baldridge, and Yonghui Wu. Vector-quantized image modeling with improved VQ-GAN. In *ICLR*, 2022. 2, 6, 7

Lijun Yu, Yong Cheng, Kihyuk Sohn, José Lezama, Han Zhang, Huiwen Chang, Alexander G. Hauptmann, Ming-Hsuan Yang, Yuan Hao, Irfan Essa, and Lu Jiang. MAGVIT: masked generative video transformer. In *CVPR*, pp. 10459–10469, 2023. 8

Lijun Yu, Jose Lezama, Nitesh Bharadwaj Gundavarapu, Luca Versari, Kihyuk Sohn, David Minnen, Yong Cheng, Agrim Gupta, Xiuye Gu, Alexander G Hauptmann, Boqing Gong, Ming-Hsuan Yang, Irfan Essa, David A Ross, and Lu Jiang. Language model beats diffusion - tokenizer is key to visual generation. In *ICLR*, 2024a. [2](#), [3](#), [4](#), [5](#), [6](#), [7](#), [8](#)

Qihang Yu, Mark Weber, Xueqing Deng, Xiaohui Shen, Daniel Cremers, and Liang-Chieh Chen. An image is worth 32 tokens for reconstruction and generation. *arXiv preprint arXiv:2406.07550*, 2024b. [6](#)

Richard Zhang, Phillip Isola, Alexei A. Efros, Eli Shechtman, and Oliver Wang. The unreasonable effectiveness of deep features as a perceptual metric. In *CVPR*, pp. 586–595, 2018. [5](#)

Susan Zhang, Stephen Roller, Naman Goyal, Mikel Artetxe, Moya Chen, Shuohui Chen, Christopher Dewan, Mona T. Diab, Xian Li, Xi Victoria Lin, Todor Mihaylov, Myle Ott, Sam Shleifer, Kurt Shuster, Daniel Simig, Punit Singh Koura, Anjali Sridhar, Tianlu Wang, and Luke Zettlemoyer. OPT: open pre-trained transformer language models. *arXiv preprint arXiv:2205.01068*, 2022. [6](#)